PAPER

Feasibility of cerium-doped LSO particles as a scintillator for x-ray induced optogenetics

Journal of Neural Engineering

RECEIVED
12 October 2020

REVISED
21 February 2021

ACCEPTED FOR PUBLICATION
17 March 2021

PUBLISHED
27 April 2021

PAPER

Feasibility of cerium-doped LSO particles as a scintillator for x-ray induced optogenetics

Aundrea F Bartley[1,3,4,5], Máté Fischer[8], Micah E Bagley[2], Justin A Barnes[2], Mary K Burdette[9], Kelli E Cannon[6], Mark S Bolding[7], Stephen H Foulger[9,10,11], Lori L McMahon[2,3,4,5], Jason P Weick[8] and Lynn E Dobrunz[1,3,4,5,*]

[1] Department of Neurobiology, University of Alabama at Birmingham, Birmingham, AL, United States of America
[2] Department of Cell, Developmental, and Integrative Biology, University of Alabama at Birmingham, Birmingham, AL, United States of America
[3] Civitan International Research Center, University of Alabama at Birmingham, Birmingham, AL, United States of America
[4] Evelyn F. McKnight Brain Institute, University of Alabama at Birmingham, Birmingham, AL, United States of America
[5] Comprehensive Neuroscience Center, University of Alabama at Birmingham, Birmingham, AL, United States of America
[6] Department of Vision Science, University of Alabama at Birmingham, Birmingham, AL, United States of America
[7] Department of Radiology, University of Alabama at Birmingham, Birmingham, AL, United States of America
[8] Department of Neurosciences, University of New Mexico-Health Sciences Center, Albuquerque, NM, United States of America
[9] Department of Materials Science and Engineering, Clemson University, Anderson, SC, United States of America
[10] Center for Optical Materials Science and Engineering Technologies, Clemson University, Anderson, SC, United States of America
[11] Department of Bioengineering, Clemson University, Clemson, SC, United States of America
[*] Author to whom any correspondence should be addressed.

E-mail: dobrunz@uab.edu

Keywords: radioluminescent, scintillator, optogenetics, x-rays, OptoXR, channelrhodopsin-2

Abstract

Objective. Non-invasive light delivery into the brain is needed for *in vivo* optogenetics to avoid physical damage. An innovative strategy could employ x-ray activation of radioluminescent particles (RLPs) to emit localized light. However, modulation of neuronal or synaptic function by x-ray induced radioluminescence from RLPs has not yet been demonstrated. *Approach.* Molecular and electrophysiological approaches were used to determine if x-ray dependent radioluminescence emitted from RLPs can activate light sensitive proteins. RLPs composed of cerium doped lutetium oxyorthosilicate (LSO:Ce), an inorganic scintillator that emits blue light, were used as they are biocompatible with neuronal function and synaptic transmission. *Main results.* We show that 30 min of x-ray exposure at a rate of 0.042 Gy s^{-1} caused no change in the strength of basal glutamatergic transmission during extracellular field recordings in mouse hippocampal slices. Additionally, long-term potentiation, a robust measure of synaptic integrity, was induced after x-ray exposure and expressed at a magnitude not different from control conditions (absence of x-rays). We found that x-ray stimulation of RLPs elevated cAMP levels in HEK293T cells expressing OptoXR, a chimeric opsin receptor that combines the extracellular light-sensitive domain of rhodopsin with an intracellular second messenger signaling cascade. This demonstrates that x-ray radioluminescence from LSO:Ce particles can activate OptoXR. Next, we tested whether x-ray activation of the RLPs can enhance synaptic activity in whole-cell recordings from hippocampal neurons expressing channelrhodopsin-2, both in cell culture and acute hippocampal slices. Importantly, x-ray radioluminescence caused an increase in the frequency of spontaneous excitatory postsynaptic currents in both systems, indicating activation of channelrhodopsin-2 and excitation of neurons. *Significance.* Together, our results show that x-ray activation of LSO:Ce particles can heighten cellular and synaptic function. The combination of LSO:Ce inorganic scintillators and x-rays is therefore a viable method for optogenetics as an alternative to more invasive light delivery methods.

1. Introduction

Optogenetics is a tool that has allowed the neuroscience community to expand our understanding about individual neuronal cells and specific brain circuits during behavior and in various disease states [1–9]. The use of various types of light activated ion channels is a fundamental aspect of optogenetics to either cause membrane potential depolarization or hyperpolarization to induce or suppress action potential firing, respectively. As with all techniques, improvements to the method are constantly being developed [9–12] and there is a need for less invasive methods of light delivery to the brain *in vivo*. The most common approach requires implantation of fiber optic waveguides (fibers) or light emitting diodes (LEDs) which are several hundred microns in size and cause damage to delicate brain tissues and multiple brain regions when implanted into deep brain structures [13–15]. Often the targeted population of cells spans several cubic millimeters, requiring the light emitting devices to be positioned relatively far from the region of interest. This limitation, combined with the fact that brain tissue absorbs and scatters light, requires relatively high light intensities to be produced by the light source. This enhanced illumination can cause increases in local temperatures [16] with the consequence of increasing neuronal firing rates [17]. Clearly, technological advances are needed to provide less invasive options for light delivery for synaptic circuit control for *in vivo* optogenetics [12, 18].

One potential strategy for less invasive light delivery to the brain is the use of x-rays to activate radioluminescent materials [18–21] located within the brain. Radioluminescence is produced when a scintillating material absorbs ionizing radiation and re-emits a portion of the absorbed energy as visible light. Radioluminescent particles (RLPs) are developed from inorganic scintillator material that can emit light at various wavelengths based upon their composition. The use of RLPs would allow the light to be generated locally, overcoming the issue of light attenuation and the need for high power intensities. Additionally, inorganic scintillators can be noninvasively delivered to specific brain regions using focused ultrasound [22]. A common inorganic scintillator is Cerium-doped lutetium oxyorthosilicate (LSO:Ce). LSO:Ce material has a high light output [23, 24], and its x-ray activation has been shown to emit wavelengths of light needed to activate channelrhodopsin-2 (ChR2) [24]. Previously, we showed that LSO:Ce particles had minimal effects on neuronal function and synaptic transmission [21]. Together, these properties make LSO:Ce an ideal material to determine if radioluminescence from RLPs generated by x-ray exposure can activate ChR2 to modulate synaptic circuits.

X-rays are able to penetrate the skull and reach deep brain structures without causing damage. As a result, x-rays applied from outside the skull could be used to activate RLPs in the brain, thus locally producing light needed to activate light-sensitive effectors such as ChR2. This would remove the need for implanted LEDs, reducing physical damage to brain tissue. However, X–irradiation can impair neurogenesis with prolonged exposure [25, 26]. Little is known about how x-ray exposure affects synaptic transmission and circuit function, especially with acute applications. At the neuromuscular synapse, a high dose of x-rays has been shown to diminish synaptic transmission [27]. Additionally, a high dose of x-rays causes impairment in memory formation related to dysfunction at the synaptic level, and not only due to alterations in neurogenesis [28]. The level of exposure that would be needed for a non-invasive optogenetic technique to work and its effect on circuit function is unknown.

Here we demonstrate that a 30 min x-ray exposure (<80 Gy) had no effect on basal synaptic excitatory field potentials (fEPSPs) at hippocampal CA3-CA1 synapses. The use of x-rays did not impair induction or expression of long-term potentiation (LTP). Importantly, we demonstrate that light emitted from LSO:Ce microparticles following x-ray exposure is able to activate ChR2 and modulate cellular and synaptic function. Together, these results show that radioluminescence from LSO:Ce RLPs is capable of modulating synaptic activity at x-ray levels that are not detrimental to synaptic function. Therefore, the use of RLPs and x-rays shows potential as a less invasive method of light delivery to the brain for *in vivo* optogenetics.

2. Materials and methods

2.1. Animals

Approval was obtained for all experimental protocols from the University of Alabama at Birmingham and University of New Mexico Institutional Animal Care and Use Committees. All experiments were conducted in accordance with the Guide for the Care and Use of Laboratory Animals adopted by the National Institutes of Health. C57Bl/6J mice were housed in a 22 ± 2 °C room with food and water ad libitum. Four-week-old C57Bl/6J mice were purchased from JAX Labs (JAX# 000664) for slice electrophysiology experiments. For a subset of experiments, adult Emx:ChR2 mice were used. These mice had expression of channelrhodopsin-2 (ChR2) in excitatory neurons, which was accomplished by crossing Emx-cre mice (B6.129S2-Emx1$^{tm1(cre)Krj}$/J, JAX# 005628) [29] with floxed ChR2/EYFP mice (Ai32 (RCL-ChR2 (H134R)/EYFP, JAX# 012569)) [30]. Emx:ChR2 mice were housed in a 26 ± 2 °C room with food and water ad libitum. Mice were housed with the whole litter until weaned (P23). Weaned mice were housed with no more than seven mice in a cage. Mouse genotypes were determined from tail biopsies using real

time PCR with specific probes designed for cre and EYFP (Transnetyx, Cordova, TN).

2.2. Primary hippocampal neuronal cultures

Hippocampal cultures were made using previously established methods [31]. Briefly, brains from P0 to P1 C57Bl/6J pups (The Jackson Laboratory, Bar Harbor, ME) were isolated, and the hippocampus was dissected in ice-cold Hanks' balanced salt solution (HBSS) solution (Sigma, St. Louis, MO) supplemented with 20% FBS and $NaHCO_3$ (4.2 mM), HEPES (1 mM; Sigma), pH 7.4. Dissected hippocampi were digested for 10 min with 0.25% Trypsin (Thermo Fisher Scientific), then washed and dissociated using fire polished Pasteur pipettes of decreasing diameter in ice cold HBSS containing DNase (1500 U; Sigma). The cells were pelleted, resuspended in plating media and plated at a density of 4–5 $\times$ 10^5 cells/12 mm coverslip (Electron Microscopy Sciences, Hatfield, PA) coated with poly-Ornithine (0.1 mg ml^{-1}; Sigma; Cat.# 4638) and laminin (5 μg ml^{-1}; Thermo Fisher Scientific). Cells were allowed to adhere for 15 min before addition of 0.5 ml of plating media containing Neurobasal supplemented with 1X B27, 2 mM Glutamax, 0.5 mg ml^{-1} Pen/Strep and 5% FBS (all from Thermo Fisher Scientific) for the first 24 h. Half of the media was removed and replaced with serum-free media after 24 h. Half of the media was removed and replaced after 48 h supplemented with 4 μM cytosine 1-β-d-arabinofuranoside (Ara-C; Sigma). Neurons were fed by replacing half the volume of spent media with fresh media without serum or Ara-C every week thereafter.

2.3. Viral production and transduction

Lentivirus was produced in HEK293T cells using calcium phosphate transfection of a 15 μg total mixture of lentiviral targeting vector (Syn-ChR2(H134R)-mCherry [32]; referred to here as ChR2-mCherry or EF1a-DIO Opto β2-AR-EYFP [33]; referred to here as OptoXR-EYFP) and packaging plasmids psPax2 and pMD2.G (Addgene, Cat.# 12260 and Cat.# 12259 respectively) at a ratio of 3:2:1 for lentivirus production. 36–48 h post transfection lentivirus containing media was harvested and concentrated using Lenti-X concentrator (Takara, Mountain View, CA) as per manufacturer's recommendations. Viral pellets were resuspended in ice cold DMEM, aliquoted, and frozen at -80 °C until use, showing a viral titer of $>10^6$ IFU ml^{-1} as measured by Lenti-X GoStix (Takara, Mountain View, CA). To develop stably expressing OptoXR-EYFP cells, HEK293T cell cultures were transduced with OptoXR-EYFP using a multiplicity of infection (MOI) of 1. After allowing 2–3 days for the expression of the lentiviral products, HEK293T cells were dissociated and sorted via flow cytometry into EYFP-positive and negative subpopulations according to previously published methods [34]. Following cell sorting, EYFP-positive cells were plated in 10 cm dish format and propagated for subsequent assay. Neuronal cultures were transduced with ChR2-mCherry using a MOI of 1 at 5–7 days *in vitro* (DIV). Transduction efficiency was between 60% and 80% per batch.

2.4. X-ray exposure

X-ray exposure was generated by a mini-X silver target x-ray unit (Amptek, Bedford, MA) with the nozzle, collimator, and all filters removed. The unit was operated at 50 kV and 79 μA to produce a polyenergetic beam of x-rays. The distance between the sample and the actual x-ray source was approximately 3–3.5 cm. The output (C) of the Mini-X was measured with a RadCal 9010 x-ray dosimeter in a RadCal 10 $\times$ 6 ionization chamber. Using the equation below, the radiation dose with the x-ray source approximately 3.5 cm from the neurons provides a radiation dose rate of 0.042 Gy s^{-1}, which is relatively close to our estimates with the dosimeter cards (see below).

$$X = \frac{C(V)\ I}{d^2}$$

where X is the radiation dose rate, I is the tube current, d is the distance from the x-ray focal spot, and C is a function of tube voltage (V), which was measured at 50 kV at a distance of 7 cm. Additionally, RADTriage50 dosimeter cards (JP Laboratories, Inc.) were used to approximate the radiation dose rate on the electrophysiology setups, which was approximately 0.05 Gy s^{-1}, consistent with the dose rate calculated above.

X-rays were applied for 30 min before the application of the high frequency stimulation (HFS) protocol used to induce LTP. For activation of ChR2 experiments in primary neuronal cultures, spontaneous excitatory postsynaptic currents (sEPSCs) were recorded for 30 s without x-rays and then x-rays were applied for 30 s, and this cycle was repeated three times. For experiments looking at the activation of ChR2 in acute hippocampal slices, the pattern was 2 min of recording without x-rays followed by 2 min with x-rays, repeated three times.

The x-ray radioluminescence spectrum of the LSO:Ce microparticles was obtained using a fiber bundle (Oriel) connected to a MicroHR monochromator (Horiba Jobin Yvon) equipped with a CCD detector (Synapse). The sample was irradiated with a Mini-X x-ray tube (Amptek Inc., MA, USA) equipped with a silver target operating at a tube voltage of 50 kV and a tube current of 79 μA. The signal was collected on a grating with 300 line mm^{-1} and a blaze of 600 nm with an exposure time of 1.2 s.

2.5. Whole cell recordings from cultured neurons

Whole cell voltage clamp recordings of cultured hippocampal neurons were performed as previously described [31] with minor modifications. The extracellular solution was a modified HBSS that

contained (in mM): 140 NaCl, 3 KCl, 2 $CaCl_2$, 1 $MgCl_2$, 15 HEPES, and 23 glucose, pH 7.4, 300 mOsm. Recording pipettes with resistances of 3–5 MΩ were filled with an intracellular recording solution containing the following (in mM): 121 K-gluconate, 20 KCl, 2 $MgCl_2$, 10 EGTA, 10 HEPES acid, 2 Mg^{2+}-ATP, 0.2 Na^{+}-GTP, pH 7.2, 290 mOsm. Neurons were visualized using an Olympus Optical BX51WI microscope (Olympus Corp., Tokyo, Japan) with differential interference contrast optics at 40×. Recordings were obtained using a MultiClamp 700B amplifier (Molecular Devices, Sunnyvale, CA), filtered at 4 kHz and sampled at 100 kHz using a Digidata 1322 A analog-to-digital converter (molecular devices). Whole-cell capacitance was fully compensated but series resistance was not compensated. Access resistance was monitored before and after recordings, and cells with resistances greater than 20 MΩ at either point were discarded from analyses. sEPSCs were recorded in the absence of tetrodotoxin but Picrotoxin (50 μM; Tocris, Bristol, UK) was bath applied in the external solution to isolate excitatory currents. Based on our past experimental experiences using opsins in cell culture, the channel opening kinetics of ChR2 can look similar to a synaptic event and could therefore confound our analysis of synaptic activity; we therefore recorded only from cells not expressing ChR2. sEPSCs were measured using a holding potential of −70 mV and all recordings were performed at 32 °C. sEPSCs were analyzed using MiniAnalysis software (Synaptosoft, Fort Lee, NJ). 10 μl of LSO:Ce doped RLP solution was applied to coverslips containing cultured neurons immediately prior to recording. As the particles do not readily wash off, the final concentration of LSO:Ce RLPs was between 0.1 and 0.5 mg ml^{-1}. It is important to note that clustering of the particles made it difficult to visualize cells near the particles and there were concerns about the particles blocking the recording pipette. As a result, cells were recorded at a distance from where the particles were applied. The x-ray protocol was applied 2 min after start of whole-cell recording (break in), to allow perfusion with the internal solution.

2.6. Electrophysiology in acute hippocampal slices

2.6.1. Mouse hippocampal slice preparation

Young adult male C57Bl/6J mice (age 4 weeks; JAX# 000664) were anesthetized with isoflurane, decapitated, and brains removed; 400 μm coronal slices from dorsal hippocampus were made on a VT1000P vibratome (Leica Biosystems) in oxygenated (95%O_2/5%CO_2) ice-cold high sucrose cutting solution (in mm as follows: 85.0 NaCl, 2.5 KCl, 4.0 $MgSO_4$, 0.5 $CaCl_2$, 1.25 NaH_2PO_4, 25.0 glucose, 75.0 sucrose). After cutting, slices were held at room temperature with continuously oxygenated standard artificial cerebral spinal fluid (aCSF) (in mm as follows: 119.0 NaCl, 2.5 KCl, 1.3 $MgSO_4$, 2.5 $CaCl_2$, 1.0 NaH_2PO_4, 26.0 $NaHCO_3$, 11.0 glucose).

Male and female Emx:ChR2 mice, 3–7 months of age, were anesthetized with isoflurane and sacrificed by decapitation using a rodent guillotine. The brains were rapidly removed and placed in ice cold dissection solution containing the following (in mM): 135 N-Methyl-D-glucamine, 1.5 KCl, 1.5 KH_2PO_4, 0.5 $CaCl_2$, 3.5 $MgCl_2$, 23 $NaHCO_3$, 0.4 l-Ascorbic acid, and ten glucose, bubbled with 95% O_2/5% CO_2, pH 7.35–7.45, and osmolarity 295–305 [35]. This dissection solution has been shown to improve slice health for older age animals [36]. A vibratome (Campden 7000smz-2, Lafayette Instrument) was used to cut 300 μM thick hippocampal brain slices. The slices were maintained in oxygenated recovery solution containing (in mM) 120 NaCl, 3.5 KCl, 0.7 $CaCl_2$, 4.0 $MgCl_2$, 1.25 NaH_2PO_4, 26 $NaHCO_3$, and ten glucose and kept at room temperature. Slices were stored at room temperature in a humidified oxygenated interface recovery chamber in 2 mL of solution on top of a piece of filter paper and bubbled with 95% O_2/5% CO_2 for >1.5 h before recording.

2.6.2. Incubation of LSO:Ce microparticles with acute hippocampal slices

Acute hippocampal slices were allowed to recover for an hour before application of either vehicle (aCSF) or 0.125–0.5 mg ml^{-1} of LSO:Ce radioluminescent microparticles. This is an underestimate of the concentration of the particles on the slice as they do not evenly distribute in the solution. The slices were incubated with and without LSO:Ce microparticles for at least 30 min.

2.6.3. Electrophysiology-field recordings

Slices were interleaved between with and without x-ray exposure to control for possible changes in slice health during the recordings. Extracellular field excitatory postsynaptic potentials (fEPSPs) were recorded from the dendritic region in hippocampal area CA1 using a submersion chamber perfused with standard aCSF at 24 °C–25 °C. All data were obtained using the electrophysiology data acquisition software pClamp10 (Molecular Devices, LLC, Sunnyvale, CA.) and analyzed using Clampfit within the pClamp10 suite, and Graphpad Prism 7 (GraphPad Software, Inc.). For CA3–CA1 synapses, Schaffer collateral axons were stimulated using a twisted insulated nichrome wire electrode placed in CA1 stratum radiatum within 200–300 μm of an aCSF-filled glass recording electrode. Baseline fEPSPs were obtained by delivering stimulus pulses with a 100 μs pulse duration applied at 0.1 Hz to generate fEPSPs between 0.3 and 0.4 mV in amplitude. Only experiments with ⩽10% baseline variance were included in the final data sets. In addition, paired-pulse facilitation characteristic of this synapse [37] was recorded by applying pairs of stimulation delivered at a 50 ms

interstimulus interval (ISIs). The paired pulse ratio (PPR) was calculated by dividing the initial slope of the second fEPSP by the initial slope of the first fEPSP.

2.6.4. Long-term potentiation

At CA3–CA1 synapses, following a 20 min stable baseline (0.1 Hz, 100 μs pulse duration, with stimulation intensity set to elicit initial fEPSP amplitude of 0.3–0.4 mV), NMDA receptor-dependent LTP was induced using high-frequency stimulation (HFS, 100 Hz, 0.5 s duration, repeated five times at a 20 s interval). The fEPSP slopes were normalized to baseline.

2.6.5. Whole cell electrophysiology recording in acute hippocampal slices

For the recordings, slices were placed in a submersion recording chamber and perfused (3–4 ml min^{-1}) with aCSF. Experiments were performed at 28 °C–32 °C. For spontaneous EPSC (sEPSC) recordings, CA1 pyramidal cells were blindly patched on a Zeiss Examiner A1 upright microscope. Neurons were patched in the voltage-clamp configuration and recorded at a holding potential of −60 mV using a Multiclamp 700 A amplifier (molecular devices). Patch electrodes (4–6 MΩ) were filled with a potassium gluconate based internal solution composed of the following (in mM): 130 K-gluconate, 0.1 EGTA, 20 KCl, 2 $MgSO_4 \cdot 7H_2O$, 10 HEPES, 5 phosphocreatine-tris, 10 ATP, and 0.3 GTP. The pH was adjusted to 7.2 with KOH and osmolarity was 290–295 mOsm. The access resistance and holding current (<200 pA) were monitored continuously. Recordings were rejected if either access resistance or holding current increased ⩾25% during the experiment. Clustering of the particles on the surface of the slice made it difficult to visualize cells near the particles. Additionally, there were concerns that the LSO:Ce particles would block the recording pipette. Therefore, cells were recorded at a distance from where the particles were applied.

The holding current was analyzed at multiple time points for each x-ray cycle. Baseline measurements occurred approximately 1 and 5 s before x-ray exposure. Holding current measurements during x-ray exposure occurred approximately 1, 5, and 10 s after the start of the x-ray unit. For analysis, the difference in the holding current was taken at each interval relative to holding current at 1 s prior to start of x-ray (Δ Holding current = condition − 1 s prior to x-ray).

Analysis of sEPSC frequency and amplitude were performed using custom software written in visual basic, which measured amplitude and interevent interval. Events were fit to a template response and all events that fit the template and passed visual inspection were included in the analysis. The first 10 s of x-ray exposure was excluded from analysis as this was during the ramp up time of the mini-X unit. Additionally, the 20 s after the mini-X was turned off were excluded from analysis.

2.7. Intracellular cAMP concentration assay

Prior to performing the cAMP-Glo Assay (Promega, Cat.# V1502, Madison, WI) 20 000 HEK cells with stable expression of OptoXR-were suspended per well in a 96 well plate for treatment. A negative control group, not exposed to light during the duration of the experiment, established a baseline measurement of intracellular cAMP concentration. Exposures with either blue (470 nm) LED light (5 s; 1 mW mm^{-2}) or x-ray in the presence of LSO:Ce particles (2 min) were conducted, followed by immediate lysis of the cells to preserve cAMP from degradation after stimulation. To ensure that x-ray emission alone was insufficient to induce intracellular cAMP, an x-ray exposure (2 min) without LSO:Ce RLPs was also performed. Relative light units were measured from the cell lysates following addition of a cAMP-dependent luciferase reagent in a Tecan Infinite F200 Microplate Reader. cAMP concentrations were calculated based on a cAMP standard curve according to manufacturer instructions.

2.8. Materials

Commercial lutetium oxyorthosilicate particles (median particle size: 4 μm) were purchased from Phosphor Technologies and were doped with cerium at a 1–10 at.% cerium (LSO:Ce). Prior to their use, the particles were washed with deionized water and vacuum air dried.

2.9. Statistics

All statistics were performed with Origin software (Origin Lab Corporation, 2002) or Microsoft Excel. Data are presented as mean ± standard error of mean. Samples sizes (n) refer to either cell or slice number for electrophysiological experiments. For most electrophysiology experiments, statistical comparisons were made using either student's t-test or two-way ANOVA followed by a Tukey post hoc test. In the case of the cAMP concentration assay and the holding current measurements, a one-way ANOVA was used to determine significance. In the case of the cumulative frequency plots for sEPSCs, the Kolmogorov–Smirnov test was used to determine significance. Significance was determined as being $p < 0.05$.

3. Results

3.1. Synaptic transmission is not affected by acute application of x-rays

Little is known about the consequences of acute x-ray exposure on synaptic function and long-term plasticity. So first, we asked if basal synaptic transmission is altered by acute application of x-rays. We recorded extracellular dendritic fEPSPs from CA1 pyramidal cells in stratum radiatum in response to CA3 Schaffer

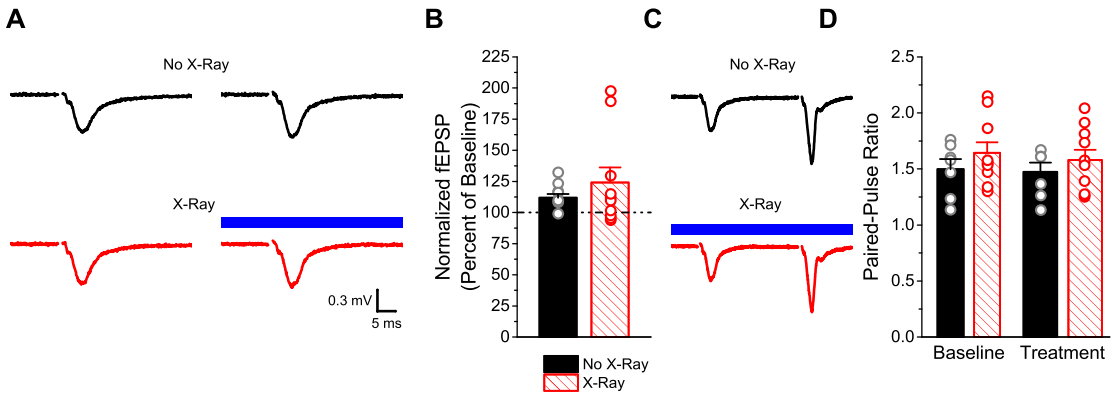

Figure 1. X-ray exposure has no effect on basal synaptic transmission. (A) Example traces of fEPSPs in response to Schaffer collateral stimulation in acute hippocampal slices for the two conditions. The top traces (black) are from a slice that was never exposed to x-rays. The bottom traces (red) are from a slice that was exposed to x-rays for 30 min after a stable baseline was obtained. The left trace is taken at the end of a 30 min baseline period for each condition. The right trace is with (bottom) and without (top) x-ray exposure, taken 30 min after the end of the baseline period. (B) No change in the basal synaptic transmission with a 30 min x-ray exposure ($n = 7, 10$; t-test; $p > 0.05$). (C) Example fEPSPs traces of paired pulses at 50 ms interval with and without a 30 min x-ray exposure. (D) No change in the paired-pulse ratio following a 30 min exposure to x-rays ($n = 7, 10, 7, 10$; ANOVA; $F_{(3,30)} = 0.046$, $p = 0.83$).

collaterals stimulation (figure 1(A)). For each experiment, a stable 30 min baseline was obtained and then the slices were exposed to either 30 min of x-rays (0.042 Gy s^{-1}) or unexposed (no x-rays) for the same amount of time. The initial slope of the fEPSP, representing glutamatergic postsynaptic response, was measured continuously throughout the experiments. We found no change in the fEPSP slope before or during x-ray exposure compared to unexposed controls (figure 1(B)). In addition, x-ray exposure elicited no change in the PPR, an indirect measure of presynaptic glutamate release [38], (figures 1(C) and (D)). Altogether, our data suggest that at this x-ray dosage (∼76 Gy) there are no significant effects on basal synaptic transmission.

3.2. LTP is inducible after an acute, continuous exposure to x-rays

Next, we asked if long-term plasticity, a mechanism required for normal learning and memory, is compromised by 30 min, continuous exposure to x-rays. LTP, an increase in synaptic strength that can last for hours *in vitro* to days when generated *in vivo*, has been extensively characterized at Schaffer collateral synapses onto CA1 pyramidal cells [39, 40]. We recorded extracellular fEPSPs in response to Schaffer collateral stimulation in an interleaved fashion where experiments from x-ray exposed and unexposed slices were alternated. Following establishment of a 30 min baseline of recording fEPSPs, slices were exposed to either 30 min of x-rays (0.042 Gy s^{-1}) or no x-rays, followed by delivery of a HFS (HFS, 100 Hz for 0.5 s, five times, separated by intervals of 20 s) to the Schaffer collaterals to induce LTP at CA3-CA1 synapses. This protocol produced identical post-tetanic potentiation and LTP magnitude in both x-ray exposed and unexposed slices. Indeed, no significant difference in LTP expression at 20 or 40 min post-tetanus in the x-ray exposed versus control slices was observed (figure 2). Our data show that LTP is still inducible after an acute, continuous exposure to x-rays.

3.3. X-ray exposure does not directly activate ChR2

Several photosensitive proteins can be activated by x-rays exposure [41, 42], especially ones that respond to UV light [43]. Channelrhodopsin-2 (ChR2), a light-gated cation channel, can be activated by wavelengths in the UV range [21], as well as visible light [44]. However, it is unknown if ChR2 can be directly activated by acute x-ray exposure. To investigate this we used Emx: ChR2 mice, in which ChR2 is expressed in all excitatory pyramidal cells, to determine if ChR2 can be directly activated by x-rays. Whole-cell voltage clamp recordings of CA1 pyramidal cells that express ChR2 were obtained, and the holding current was measured before and during the x-ray application (2 min each, 3 cycles, ∼15 Gy total, figure 3(A)). Activating ChR2 allows the influx of positive ions that would depolarize the cell and force the amount of current needed to maintain the neuron at −60 mV to change, referred to as the photocurrent. No visible photocurrent was observed during application of 0.042 Gy s^{-1} x-rays, the rate of exposure performed in these experiments (figure 3(B)). Additionally, this was verified by measuring the change in the holding current at multiple time points at the beginning of the x-ray application. There was no significant effect on the holding current in ChR2 expressing neurons in the presence of x-rays as compared to baseline (no x-rays) changes (figure 3(C)). This confirms that this x-ray dose does not appear to directly activate ChR2 in the soma where the recordings are occurring.

However, x-rays might cause activation of ChR2 in either axons or dendrites thereby altering synaptic

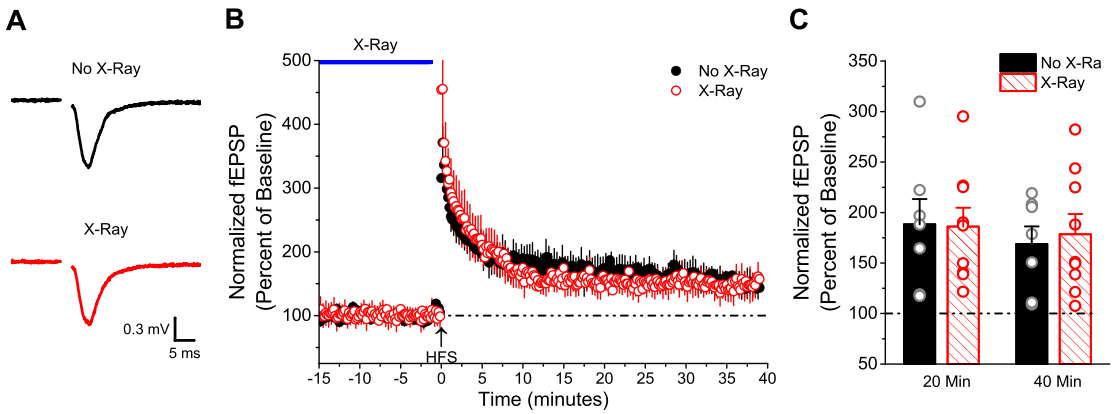

Figure 2. Prolonged, continuous x-ray does not prevent the induction of LTP. (A) Averaged representative fEPSP trace at 35 min post-HFS stimulation with and without 30 min x-ray exposure. (B) Induction of HFS LTP was similar between groups ($n = 7, 9$; t-test; $p > 0.05$). (C) No difference in the LTP magnitude at either 20 or 40 min after induction with x-ray exposure ($n = 7, 9$; t-test; $p > 0.05$).

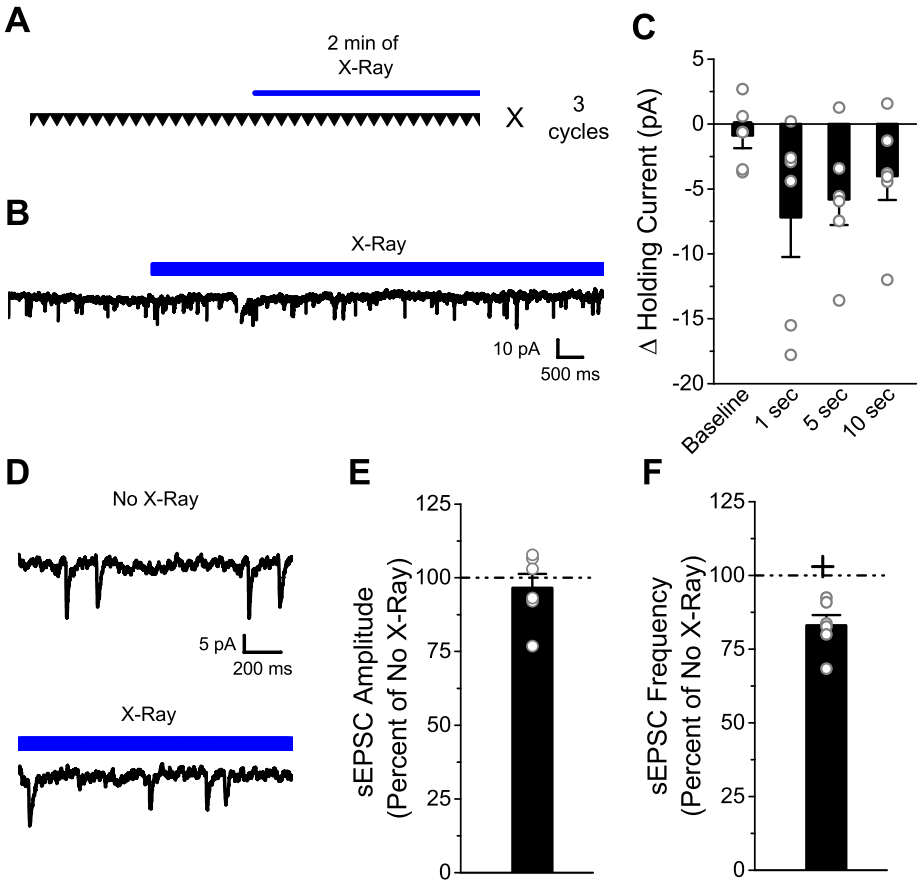

Figure 3. X-ray exposure does not directly activate ChR2. (A) Schematic of experimental paradigm. (B) Example traces showing that there was no photocurrent induced by x-ray exposure in neurons that express ChR2. The electrical artifact from the mini-X was removed from the trace, it spanned approximately a 100 ms. (C) No alteration in the amount of holding current needed to keep the PC at −60 mV ($n = 6$; ANOVA; $F_{(3,23)} = 1.67$, $p = 0.21$). All values are measured relative to the individual cell's holding current at 1 s prior to the start of x-ray; baseline is measured 5 s prior to start of x-ray. (D) Example traces of sEPSCs onto CA1 PCs from Emx: ChR2 slices in the presence or absence of x-rays. (E) No change in the sEPSC amplitude with x-ray exposure ($n = 6$; t-test; $p = 0.3$). (F) Minor decrease in the number of sEPSC events in the presence of x-rays ($n = 6$; t-test; $p = 0.005$). + indicates significant difference between no x-ray and x-ray exposure.

transmission. Therefore, we analyzed sEPSCs onto ChR2 expressing neurons. As there is cell to cell variability with sEPSCs, we used a within cell control (no x-ray) to normalize the amplitude and frequency of sEPSCs. Figure 3(A) depicts the experimental paradigm showing that the periods of x-ray exposure and no exposure were interleaved throughout the course of the experiment. No change in the amplitude

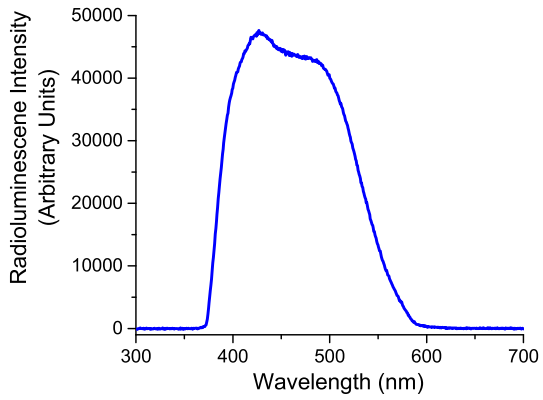

Figure 4. LSO:Ce microparticle emission is in range to activate ChR2. Emission spectrum of LSO:Ce microparticles in response to x-ray exposure. The peak emission of LSO:Ce microparticles is approximately 420 nm. ChR2 peak activation wavelength is around 450 nm.

of sEPSCs was observed, but there was a minor decrease in the frequency of sEPSCs with the application of x-rays. Together, the data provide strong evidence that x-rays are not able to directly activate ChR2.

3.4. LSO:Ce radioluminescence is appropriate for ChR2

ChR2 has been shown to be activated by wavelengths between 350 and 525 nm, with a peak at 470 nm [21, 45]. Previously, we demonstrated that radioluminescent LSO:Ce microparticles are biocompatible with neuronal health and function [21], and thus potentially useful for x-ray optogenetics. LSO:Ce has been widely studied as a scintillator, and has been shown to emit visible light in response to x-rays [46–48]. The LSO host lattice provides two potential Lu^{3+} sites that Ce^{3+} can substitute, with the Ce1 site surrounded by seven oxygen neighbors while the Ce2 site has six oxygen neighbors. The relaxation of electrons from the 5d to 4f states of cerium from these two sites creates a broad radioluminescence emission that spans between 370 and 590 nm [49]. We confirmed the emission spectrum for the 4 μm LSO:Ce microparticles in response to x-rays from the mini-X used in our experiments with a fiber bundle connected to a MicroHR monochromator. Figure 4 shows that LSO:Ce particles emit visible light in response to x-rays over wavelengths from 370 to 590 nm, which is well within the appropriate range to activate ChR2.

3.5. X-ray induced LSO:Ce radioluminescence stimulates G-protein coupled receptor (GPCR) activity

We first tested *in vitro* whether LSO:Ce RLPs could generate sufficient light output in response to x-rays to regulate opsin activity using a chimeric opsin receptor strategy. Of this class of chimeric receptors, collectively called OptoXRs, we utilized a chimeric fusion protein made up of the light-gated extracellular domain of rhodopsin fused to the intracellular portions of β2-adrenergic receptor (β2-AR), and tagged with a fluorescent EYFP molecule on the *C* terminus to allow for easy visualization of transgene expression (OptoXR-EYFP). In response to light activation, OptoXR-EYFP undergoes a conformational change to trigger activation of $G_{\alpha s}$ signal transduction and stimulate cyclic AMP (cAMP) production mediated by adenylyl cyclase activation [33, 50]. For these experiments, we expressed OptoXR-EYFP in HEK293T cells (figure 5(A)). We then tested whether intracellular cAMP concentrations could be increased under various stimulation conditions using a cAMP-dependent luciferase reaction as a readout (see section 2). As a positive control, we used LED stimulation in the absence of LSO:Ce RLPs, which caused a significant increase in cAMP concentration (cAMP) compared to cells that remained in dark conditions (figure 5(B)). In order to determine whether LSO:Ce radioluminescence could also increase (cAMP), we exposed HEK293T cells expressing OptoXR-EYFP to x-rays in the absence or presence of LSO:Ce RLPs. Importantly, while x-rays alone did not alter intracellular (cAMP) relative to dark control, x-ray exposure in the presence of LSO:Ce particles caused a significant increase in (cAMP) (figure 5(B)). Since cAMP is the primary downstream target of β2-adrenergic receptor activity, an enhancement in cAMP levels in the presence of x-rays and RLPs demonstrates that light emitted from the RLPs is capable of activating a chimeric opsin protein and causing downstream activation of an intracellular second messenger cascade.

3.6. X-ray induced LSO:Ce radioluminescence stimulates neuronal activity

To determine whether x-rays can alter neuronal network activity via RLP-mediated scintillation, we tested the effects in cell culture and acute brain slices, two *in vitro* systems that are widely used in studies of synaptic transmission. First, we used dissociated hippocampal neurons in culture between 16 and 18 days *in vitro* (DIV) that expressed ChR2-mCherry and were either exposed to LSO:Ce RLPs or not treated with RLPs. We recorded from neurons lacking expression of ChR2-mCherry and measured spontaneous excitatory post synaptic currents (sEPSCs) in the absence of the sodium channel blocker tetrodotoxin (TTX). These neurons received alternating 30 s periods without and with x-ray exposure which provided less than 2 Gy of x-rays to each cell (figure 6(A)). Figure 6(B) shows example traces of sEPSCs from neurons incubated with and without RLPs during periods of recordings in the presence or absence of x-rays. Figures 6(C) and (E) display pooled data for mean amplitude and frequency of sEPSCs for these conditions. Data are plotted as the ratio of recorded activity during x-ray exposure to activity

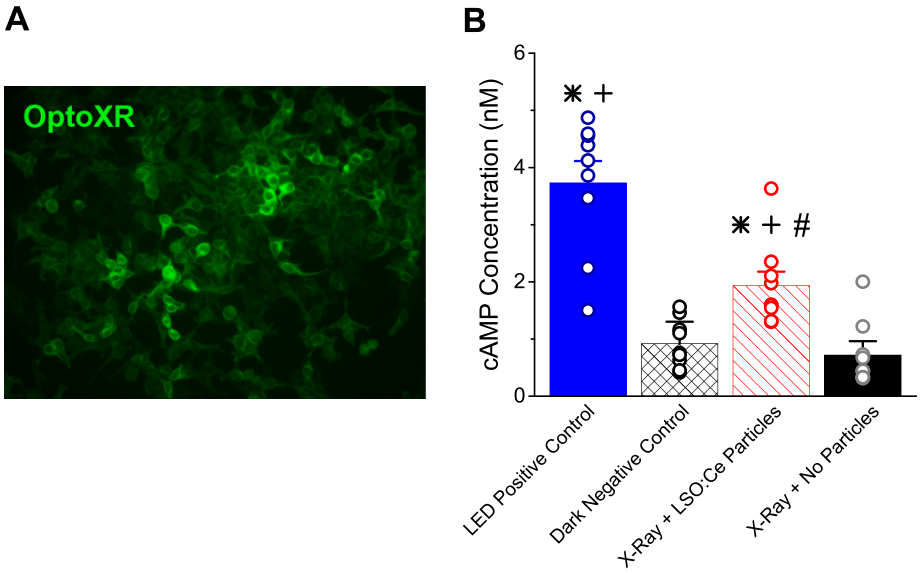

Figure 5. Radioluminescence from LSO:Ce particles induces cAMP production through light-gated β2-AR receptor (OptoXR) *in vitro*. (A) Epifluorescent image of HEK293T cells stably expressing OptoXR-EYFP. (B) The greatest intracellular cAMP concentration was measured in the LED control group, while the x-ray with RLP condition showed greater cAMP levels than either negative control conditions ($n = 9$/group; ANOVA; $F_{(3,32)} = 29.1$, $p < 0.0001$). * indicates significant difference from dark negative control ($p < 0.05$). + indicates significant difference from x-ray + no particles ($p < 0.05$). # indicates significant difference from LED positive control ($p < 0.05$).

recorded in the absence of x-ray exposure (mean of three repetitions for each condition). Figures 6(D) and (F) display the cumulative frequency plots of the sEPSC amplitudes and ISIs. Interestingly, only neurons that received x-ray exposure in the presence of LSO:Ce RLPs displayed a significant increase in sEPSC frequency (figure 6(E)), which was verified in the cumulative frequency plot of the ISIs (figure 6(F)). The amplitude of the sEPSCs potentially shows a trend for a slight increase in size with the combination of LSO:Ce RLPs and x-rays. The cumulative frequency plot of the sEPSC amplitudes was shifted slightly rightward (figure 6(D)), but the average amplitude was unchanged (figure 6(C)). Neither neurons exposed to x-rays alone nor neurons incubated with RLPs in the absence of x-ray exposure showed differences in sEPSC frequency or amplitude (figures 6(C)–(F)).

Next, we confirmed that the increase in sEPSCs using the combination of RLPs and x-rays can occur in acute hippocampal slices. We used Emx:ChR2 mice and incubated the slices with either LSO:Ce particles or vehicle, and recorded from CA1 pyramidal cells. Because we used slices from Emx:ChR2 mice, all CA1 pyramidal cells expressed ChR2. Because the particles on the slice made it difficult to visualize neurons and could block the recording pipette, cells were patched at a distance from the particles, thereby preventing us from observing an effect on holding current recorded from the soma. Figure 7(A) shows the experimental paradigm and that the neuron received alternating 2 min periods with and without x-ray exposure, thereby exposing the slice to approximately 15 Gy dose of x-rays in total. Figure 7(B) shows example traces of the sEPSCs recorded from ChR2 expressing neurons for the various conditions. We observed a small increase in the average amplitude of the sEPSCs in the presence of LSO:Ce particles and x-ray exposure (figure 7(C)), which was verified by a rightward shift in the cumulative frequency plot of the sEPSC amplitudes (figure 7(D)). This appeared to affect a range of sEPSC amplitudes, suggesting there was not an effect only on a specific population. Importantly, we also observed a significant increase in average sEPSC frequency with the combination of RLPs and x-ray exposure (figure 7(E)). Consistent with this, there was also a leftward shift in the ISIs (inverse of frequency) cumulative frequency plot (figure 7(F)), indicating a decrease in the time between synaptic events. Together, these data indicate that the x-ray induced radioluminescence from LSO:Ce particles is able to activate ChR2-expressing neurons to enhance network effects, as indicated by the increase in sEPSCs frequency and amplitude.

4. Discussion

Our results provide proof of principle that radioluminescence from scintillators can stimulate opsins and modulate synaptic function. Specifically, we show that x-ray induced visible light emission from LSO:Ce RLPs increased synaptic function via activation of ChR2, as indicated by enhanced sEPSC frequency in both cultured neurons and acute hippocampal slices. This result is consistent with the idea that the light emitted from LSO:Ce particles

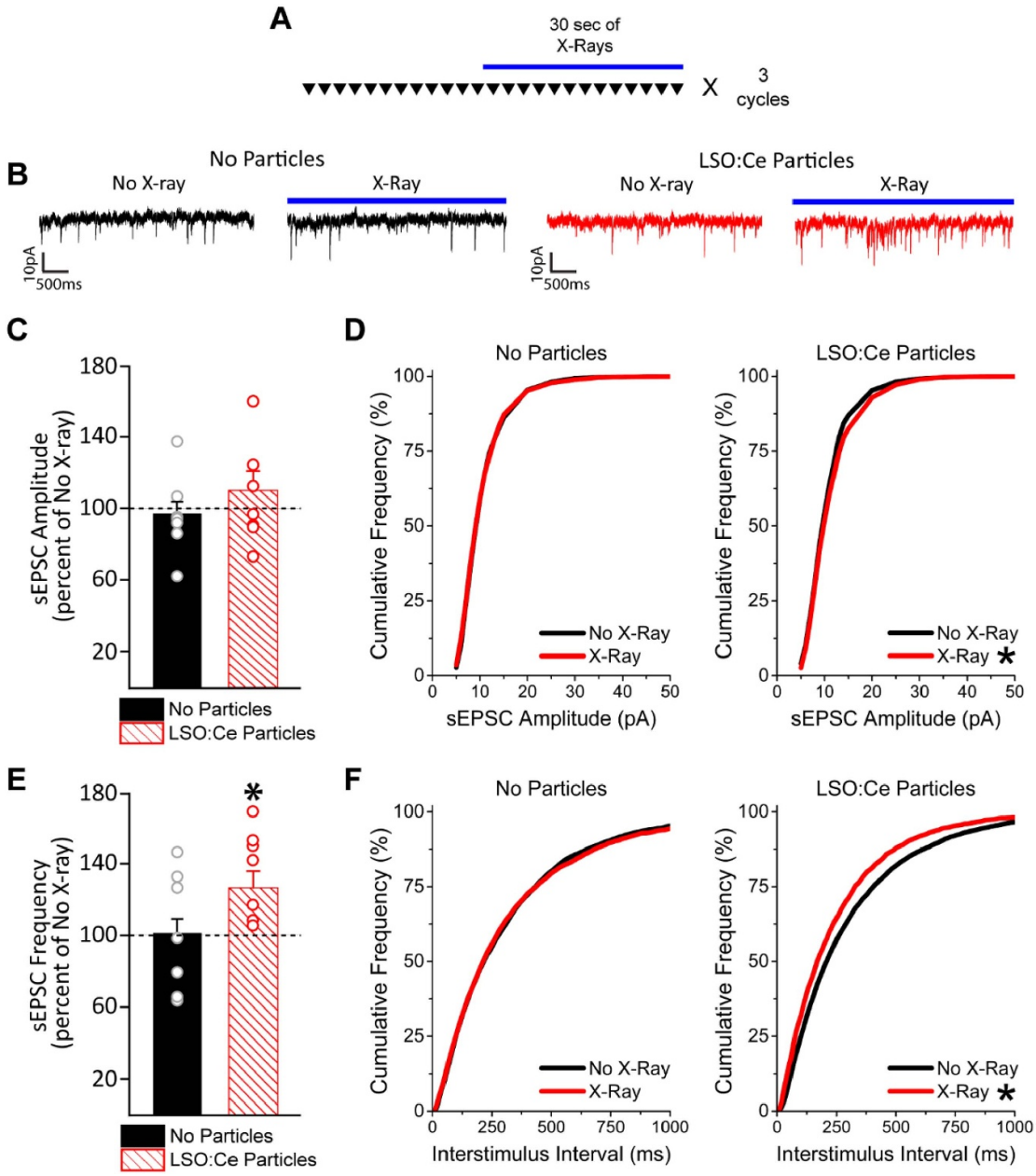

Figure 6. X-ray mediated radioluminescence from LSO:Ce particles enhances synaptic activity in primary hippocampal neuronal cultures. (A) Diagrammatic summary of experimental design using alternating exposure to x-rays or absence of x-rays for each recorded cell. (B) Representative voltage-clamp traces of sEPSCs recorded from hippocampal neurons with and without LSO:Ce particles in the presence or absence of x-rays. (C) Pooled data illustrating that 30 s x-ray exposure did not alter sEPSC amplitude either in the presence of LSO:Ce particles or in the absence of particles ($n = 7$/group; ANOVA; $F_{(3,24)} = 0.39$, $p = 0.76$). (D) Cumulative frequency distribution plots are displayed showing the frequency distribution of the sEPSC amplitudes in the presence (right graph) or absence (left graph) of LSO:Ce particles with and without x-ray exposure. There is a slight rightward shift in the distribution when both LSO:Ce particles and x-rays are present suggesting a slight increase in the amplitudes of sEPSCs in this condition ($n = 7$/group; Kolmogorov–Smirnov; $D_{(17\,810)} = 0.051$, $p < 0.05$). (E) Pooled data illustrate that exposure of cultures to x-rays in the presence of the LSO:Ce particles enhanced sEPSC frequency ($n = 7$/group; ANOVA; $F_{(3,24)} = 3.76$, $p = 0.02$) compared to periods when x-ray was turned off (dashed line). However, x-ray exposure alone did not alter the number of sEPSC events in the absence of LSO:Ce particles. (F) Cumulative frequency distribution plots are displayed showing the frequency distribution of the sEPSC interstimulus interval in the presence (right graph) or absence (left graph) of LSO:Ce particles with and without x-ray exposure. There is a leftward shift in the distribution when both LSO:Ce particles and x-rays are present showing a shorter interval between events for this condition ($n = 7$/group; Kolmogorov–Smirnov; $D_{(17\,810)} = 0.079$, $p < 0.05$). For *C* and *E* * indicates significant difference between with and without LSO:Ce particles. For *D* and *F* * indicates a significant difference between no x-ray and x-ray exposure.

in response to x-ray is effectively activating ChR2, leading to axon depolarization and increased neurotransmitter release. Additionally, we showed that the combination was able to work with a chimera opsin receptor to increase cAMP concentrations, showing some of the versatility of this system. We also demonstrate that an acute 30 min x-ray exposure does not negatively impact hippocampal basal synaptic transmission or the induction of LTP. Furthermore, we showed that ChR2 is not directly activated by

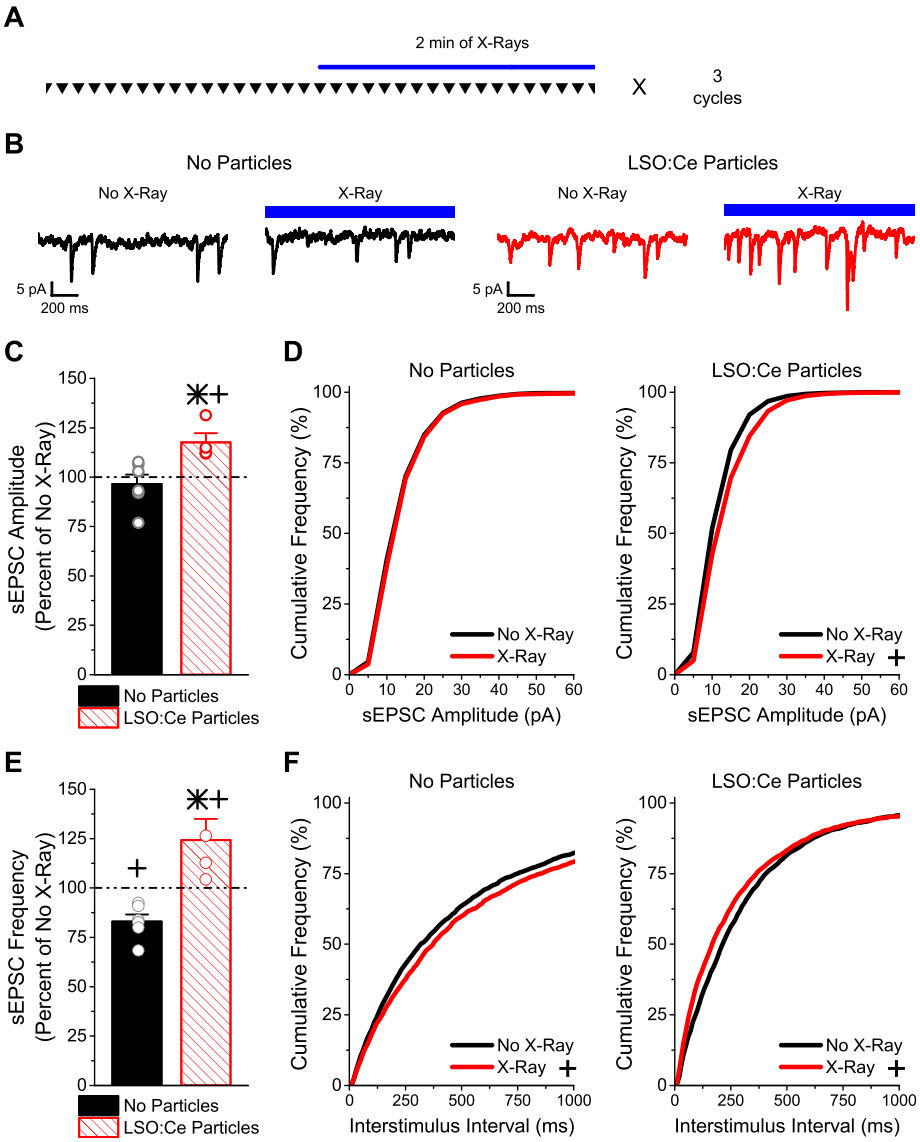

Figure 7. X-ray mediated radioluminescence from LSO:Ce particles enhances synaptic activity of ChR2-expressing neurons in acute hippocampal slices. (A) Diagrammatic summary of experimental design using alternating exposure to x-rays or absence of x-rays for each recorded cell. (B) Example sEPSC traces onto CA1 PCs in slices from Emx:ChR2 mice, incubated with and without LSO:Ce particles, in the presence or absence of x-rays. (C)–(F) X-rays plus LSO:Ce particles activated ChR2 in four out of six experiments. (C) The presence of the LSO:Ce particles enhanced the sEPSC amplitude during x-ray exposure ($n = 6, 4$; ANOVA; $F_{(3,16)} = 6.74$, $p = 0.004$). (D) Cumulative frequency distribution plots are displayed of the sEPSC amplitudes in the presence (right graph) or absence (left graph) of LSO:Ce particles with and without x-ray exposure. A rightward shift in the distribution is observed only when both LSO:Ce particles and x-rays are present showing an overall increase in the size of sEPSCs ($n = 6, 4$; Kolmogorov–Smirnov; $D_{(4823)} = 0.098$, $p < 0.05$). (E) The light emitted from LSO:Ce particles by x-ray activation increases the frequency of sEPSCs ($n = 6, 4$; ANOVA; $F_{(3,16)} = 12.35$, $p = 0.0002$). However, x-ray exposure in the absence of LSO:Ce particles reduced the frequency of sEPSCs recorded from PCs in Emx:ChR2 mice. (F) Cumulative frequency distribution plots are displayed of the sEPSC interstimulus interval in the presence (right graph) or absence (left graph) of LSO:Ce particles with and without x-ray exposure. A rightward shift in the distribution was observed when no particle slices were exposed to x-rays indicating that the time between events was slower ($n = 6$; Kolmogorov–Smirnov; $D_{(6010)} = 0.055$, $p < 0.05$). However, in the presence of the LSO:Ce particles the application of x-rays caused a leftward shift of the distribution showing that the interval between events is faster ($n = 4$; Kolmogorov–Smirnov; $D_{(4805)} = 0.097$, $p < 0.05$). * indicates significant difference between with and without LSO:Ce particles. + indicates significant difference between no x-ray and x-ray exposure.

x-rays. Together, these results suggest that the combination of x-rays and LSO:Ce particles could be suitable for *in vivo* optogenetics using ChR2.

The use of x-rays has several distinct advantages over implanted LEDs to activate ChR2 *in vivo*. One disadvantage of implanted LEDs is that brain tissue causes light scattering, therefore necessitating the use of high levels of light to activate ChR2 *in vivo*. This can cause heating of brain tissue; it has been reported that local tissue temperature increased by 0.8 °C with illumination used for optogenetics [16]. Prolonged illumination and trains of light pulses elicit even higher temperature increases in tissue [12, 17]. Heating of tissue due to illumination causes damage and contributes to behavioral changes or physiological effects [17, 51]. In contrast, application of x-rays for a

short time caused no heating in the tissue [18]. Additionally, x-rays can penetrate further (scatter less) and retain the majority of their transmission compared to near infrared and visible light [18]. The mean free path length of a 25 keV x-ray photon in brain tissue is approximately 2.1 cm [52], whereas a 453 nm (blue) photon has a mean free path length of around 0.1 mm [53]. As a result, the x-rays are about 50–100 times more penetrating than the optical photons in brain tissue. Perhaps most importantly, x-rays are much more capable of penetrating the skull, removing the need for an invasive delivery method that causes physical damage. Another advantage of combining x-rays with RLPs is that scintillators can be delivered in extremely close proximity to the cells expressing the opsins and therefore less light is needed to stimulate the opsin. Radioluminescent nanoparticles have been shown to persist in brain tissue for at least 72 h after injection [54], enabling repeated experiments over multiple days. Radioluminescent nanoparticles can also be delivered into the brain using focused ultrasound to open the blood brain barrier [22], avoiding the damage of intracranial injection. X-ray activation of RLPs is therefore a potentially viable method for noninvasive optogenetics.

Extremely high doses (>450 Gy) of x-rays have been shown to abolish nerve conduction [55, 56] and alter synaptic transmission [27]. Deficits in fear memory can occur as a result of acute x-ray exposure, independent of its effect on neurogenesis [28]. However, in our study, with a moderate dose of x-rays (<80 Gy), no effect was seen on basal synaptic transmission and LTP could still be induced. LTP was even maintained to the same level 40 min after induction. It is possible that waiting a longer time period after x-ray application might have different effects on synaptic transmission, as one study showed a transient decrease in dendritic protein levels hours after the exposure [28]. However, it is most unlikely that low doses (<10 Gy) of x-ray will influence synaptic transmission and these are levels that can be used for x-ray optogenetics, as we have shown here. In our study, we show that using less than 2 Gy of x-rays to produce scintillation from LSO:Ce particles is sufficient to cause changes in activity of ChR2-expressing neurons. It is well known that radiation can produce stochastic effects resulting in genetic changes. This would thus have a negligible influence on the results of shorter-term experiments using x-ray optogenetics in small animals in laboratory settings.

Multiple proteins can be altered and/or directly activated by x-rays, including rhodopsin [41, 57–60]. Recently, LITE-1, a UV light sensitive GPCR in C. elegans, has been discovered to also be activated by x-rays, producing behavioral effects [43]. However, to our knowledge, none of the opsins typically used for optogenetics have ever been tested for x-ray sensitivity. Several of these opsins can be activated by a wide range of wavelengths, including ChR2, which can be activated by UV as well as visible light [21]. Here we showed that in the absence of LSO:Ce microparticles, x-rays did not increase cAMP production by OptoXR or alter the holding current in neurons expressing ChR2, consistent with no direct activation of these opsins by x-rays. However, the holding current was recorded at the soma, and it is possible that a small photocurrent was induced by x-ray activation of ChR2 in the dendrites or axons that was large enough to cause localized depolarizations. But, we also saw no increase in synaptic activity during the application of x-rays alone in neurons that express ChR2. Instead, a small decrease in sEPSC frequency was observed with application of x-rays to ChR2 expressing pyramidal cells, an effect that was observed previously with the use of UV light [21]. Together, these results suggest that ChR2 and OptoXR are not directly activated by x-rays. Further studies will be needed to confirm whether this is true for other opsins used in optogenetics.

Repeated x-ray exposure has been shown to abolish neurogenesis [61, 62] and affect cognitive function, as seen for radiotherapy [63]. Neurogenesis can be diminished even with a single x-ray exposure [25, 64]. However, this is most likely due to oxidative stress and can be minimized using a free radical scavenger [65]. Low doses of x-rays had minimal to no effect on neurogenesis [64, 66]. In our studies, we did not analyze the effect on neurogenesis for the doses used, but our proof of principle experiments reported here employed doses that are in range with minimal effects on neurogenesis. A study has shown that the peak radioluminescence emission from scintillators can be increased by fine-tuning the x-ray energy [67], suggesting that activation of the LSO:Ce microparticles could occur at even lower x-ray doses.

A variety of different materials that emit light have been shown to be able to activate different opsins [12, 18, 68–70]. The idea of using x-rays together with scintillating materials to produce light for optogenetics was proposed by Berry *et al* [71], who called the potential method X-optogenetics. They surveyed several possible materials that could be used, which they referred to as nanophosphors, and materials that are used as dopants to change the emission spectra [71]. However, the appropriate material must be chosen to pair with the opsin being used. Currently, the most common opsin being used is ChR2, which has an absorption range between 400 and 500 nm. Therefore, we selected Lu_2SiO_5 doped with Ce (LSO:Ce), a scintillator that has been extensively characterized [23, 72] and used in multiple medical devices [23, 47, 73]. Cerium forms the luminescence center in LSO, and the emission spectrum (380–550 nm) makes it well suited for optogenetics applications using ChR2 [74, 75]. It has many attractive properties, including having one of the highest light outputs (25 K photons MeV^{-1}). In addition, LSO:Ce is nonhygroscopic, biologically inert, and can be

synthesized at the nanoscale level [76, 77]. While we used microparticles in this study, LSO:Ce nanoparticles could be used to increase their likelihood of passing through the blood-brain barrier, especially if used together with focused ultrasound to increase BBB permeability [22]. We previously demonstrated that LSO:Ce microparticles are non-toxic to neurons and had very minor effects on synaptic transmission [21]. In contrast, relatively little is known about how other scintillating materials effect neuronal health and synaptic transmission. One scintillator shown to be biocompatible with neurons is $Gd_3(Al,Ga)_5O_{12}$ [18]. A previous study showed that x-rays and a crystal of $Gd_3(Al,Ga)_5O_{12}$ can be used to induce circuit changes through activation of the red-shifted opsin ChRmine [18]. A limitation of this study was the large size of the crystal implanted, which was larger than a typical fiber optic and caused damage to the surrounding tissue. Additionally, there was a similar increase in active microglia with implantation of the crystal as compared to a fiber optic. However, we previously showed that the LSO:Ce microparticles had no effect on astrocytes [21]. LSO:Ce microparticles therefore have the advantage of being able to enhance synaptic transmission through x-ray induced luminescent activation of ChR2 while avoiding tissue damage that can occur with other materials.

Our current findings provide proof of principle that LSO:Ce can be used as a scintillator for x-ray induced optogenetics to modulate circuit activity. The increase in synaptic activity was reproducible and occurred in cell culture and intact slices, although the effect size was modest. Limitations include the distance of x-rays from the particles and of the particles from the opsins. X-rays can transmit at a high penetrance for several millimeters, however the x-ray output can be diminished if the target is too far from the source. In our experiments, the distance from the x-ray source to the cells was somewhat variable. This would cause some slight differences in the amount of x–irradiation that was delivered for each experiment and probably contributed to the small effect seen in our proof of principle experiments. Another limitation of our current experimental paradigm is that the particles were applied to the surface of the slice, and were therefore more than 100 μms from the cells expressing ChR2. In addition, the particles are not evenly dispersed across the slice or coverslip. This could also contribute to the modest effect of ChR2 activation observed in this study. Furthermore, because particles were not adjacent to the recorded neurons, this technical limitation prevented us from directly detecting photocurrents in the recorded cells. However, *in vivo*, delivery of RLPs across the blood brain barrier [22] disperses RLPs throughout brain tissue, potentially increasing the effect size. In addition, a different opsin with greater light sensitivity than ChR2, such as ChRmine [78], could be used in future studies in order to maximize neuronal activation by x-ray induced radioluminescence.

5. Conclusion

In summary, our results provide the first demonstration of enhanced neuronal activity by x-ray activation of radioluminescent microparticles. While further studies are needed to determine the appropriate size of LSO:Ce particles that can be used *in vivo*, as well as the necessary density required, our study supports the possibility of using radioluminescence from LSO-Ce particles caused by x-ray activation as a non-invasive way to deliver light to the brain.

Data availability statement

The data that support the findings of this study are available upon reasonable request from the authors.

Acknowledgments

This work was funded by NSF Track 2 FEC OIA-1632881 to L M, J W, and S F, and NINDS 1R01NS116051 to J W, and an Alabama State Funded EPSCoR Graduate Research Scholars Fellowship to K C. We would like to thank Dr David Gauntt for his expertise in x-ray physics.

ORCID iDs

Aundrea F Bartley https://orcid.org/0000-0002-2764-3060
Máté Fischer https://orcid.org/0000-0002-6970-5039
Lori L McMahon https://orcid.org/0000-0003-1104-6584
Lynn E Dobrunz https://orcid.org/0000-0002-3317-554X

References

[1] Emiliani V, Cohen A E, Deisseroth K and Häusser M 2015 All-optical interrogation of neural circuits *J. Neurosci.* **35** 13917–26
[2] Selimbeyoglu A *et al* 2017 Modulation of prefrontal cortex excitation/inhibition balance rescues social behavior in CNTNAP2-deficient mice *Sci. Transl. Med.* **9** 401
[3] Fenno L E, Gunaydin L A and Deisseroth K 2015 Mapping anatomy to behavior in Thy1:18 ChR2-YFP transgenic mice using optogenetics *Cold Spring Harb. Protoc.* **2015** 537–48
[4] Gunaydin L A *et al* 2014 Natural neural projection dynamics underlying social behavior *Cell* **157** 1535–51
[5] Yizhar O *et al* 2011 Neocortical excitation/inhibition balance in information processing and social dysfunction *Nature* **477** 171–8
[6] Gradinaru V, Mogri M, Thompson K R, Henderson J M and Deisseroth K 2009 Optical deconstruction of Parkinsonian neural circuitry *Science* **324** 354–9
[7] Rost B R, Schneider-Warme F, Schmitz D and Hegemann P 2017 Optogenetic tools for subcellular applications in neuroscience *Neuron* **96** 572–603

[8] Barnett S C, Perry B A L, Dalrymple-Alford J C and Parr-Brownlie L C 2018 Optogenetic stimulation: understanding memory and treating deficits *Hippocampus* **28** 457–70

[9] Lim D H, Ledue J, Mohajerani M H, Vanni M P and Murphy T H 2013 Optogenetic approaches for functional mouse brain mapping *Front. Neurosci.* **7** 54

[10] Rein M L and Deussing J M 2012 The optogenetic (r)evolution *Mol. Genet. Genomics* **287** 95–109

[11] Lin X *et al* 2017 Multiplexed optogenetic stimulation of neurons with spectrum-selective upconversion nanoparticles *Adv. Healthcare Mater.* **6** 1700446

[12] Chen S *et al* 2018 Near-infrared deep brain stimulation via upconversion nanoparticle-mediated optogenetics *Science* **359** 679–84

[13] Aravanis A M, Wang L-P, Zhang F, Meltzer L A, Mogri M Z, Schneider M B and Deisseroth K 2007 An optical neural interface: *in vivo* control of rodent motor cortex with integrated fiber optic and optogenetic technology *J. Neural. Eng.* **4** S143–56

[14] Canales A, Park S, Kilias A and Anikeeva P 2018 Multifunctional fibers as tools for neuroscience and neuroengineering *Acc. Chem. Res.* **51** 829–38

[15] Ozden I *et al* 2013 A coaxial optrode as multifunction write-read probe for optogenetic studies in non-human primates *J. Neurosci. Methods* **219** 142–54

[16] Senova S, Scisniak I, Chiang C-C, Doignon I, Palfi S, Chaillet A, Martin C and Pain F 2017 Experimental assessment of the safety and potential efficacy of high irradiance photostimulation of brain tissues *Sci. Rep.* **7** 43997

[17] Stujenske J M, Spellman T and Gordon J A 2015 Modeling the spatiotemporal dynamics of light and heat propagation for *in vivo* optogenetics *Cell Rep.* **12** 525–34

[18] Matsubara T *et al* 2019 Remote control of neural function by x-ray-induced scintillation *bioRxiv Preprint*

[19] Shuba Y M 2014 Use of scintillator-based nanoparticles for *in vivo* control of light-sensitive bioactive molecules 10183081 (Washington, DC)

[20] French D N, Cannon K, Bartley A, McMahon L and Gray G 2018 *Novel X-ray Fluorescent Organic Monomer and Polymer Materials for Optogenetic Applications. Biophotonics Congress: Biomedical Optics Congress 2018 (Microscopy/translational/brain/ots)* pp JTu3A.55

[21] Bartley A F *et al* 2019 LSO:Ce inorganic scintillators are biocompatible with neuronal and circuit function *Front. Synaptic Neurosci.* **11** 24

[22] Rich M *et al* 2020 A noninvasive approach to optogenetics using focused ultrasound blood brain barrier disruption for the delivery of radioluminescent particles *bioRxiv Preprint*

[23] Roy S, Lingertat H, Brecher C and Sarin V 2013 Optical properties of anisotropic polycrystalline Ce+3 activated LSO *Opt. Mater.* **35** 827–32

[24] Melcher C L and Schweitzer J S 1991 Cerium-doped lutetium oxyorthosilicate: a fast, efficient new scintillator *Conf. Record of the 1991 IEEE Nuclear Science Symp. and Medical Imaging Conf.* (IEEE) pp 228–31

[25] Mizumatsu S, Monje M L, Morhardt D R, Rola R, Palmer T D and Fike J R 2003 Extreme sensitivity of adult neurogenesis to low doses of X-irradiation *Cancer Res.* **63** 4021–7

[26] Cacao E, Kapukotuwa S and Cucinotta F A 2018 Modeling reveals the dependence of hippocampal neurogenesis radiosensitivity on age and strain of rats *Front. Neurosci.* **12** 980

[27] Portela A *et al* 1977 X-radiation actions on the neuromuscular transmission *Acta Physiol. Lat. Am.* **27** 157–76

[28] Puspitasari A, Koganezawa N, Ishizuka Y, Kojima N, Tanaka N, Nakano T and Shirao T 2016 X irradiation induces acute cognitive decline via transient synaptic dysfunction *Radiat. Res.* **185** 423–30

[29] Gorski J A, Talley T, Qiu M, Puelles L, Rubenstein J L R and Jones K R 2002 Cortical excitatory neurons and glia, but not GABAergic neurons, are produced in the Emx1-expressing lineage *J. Neurosci.* **22** 6309–14

[30] Madisen L *et al* 2012 A toolbox of Cre-dependent optogenetic transgenic mice for light-induced activation and silencing *Nat. Neurosci.* **15** 793–802

[31] Chander P, Kennedy M J, Winckler B and Weick J P 2019 Neuron-specific gene 2 (NSG2) encodes an AMPA receptor interacting protein that modulates excitatory neurotransmission *Eneuro* **6** ENEURO.0292-18.2018

[32] Weick J P, Liu Y and Zhang S-C 2011 Human embryonic stem cell-derived neurons adopt and regulate the activity of an established neural network *Proc. Natl Acad. Sci. USA* **108** 20189–94

[33] Airan R D, Thompson K R, Fenno L E, Bernstein H and Deisseroth K 2009 Temporally precise *in vivo* control of intracellular signalling *Nature* **458** 1025–9

[34] Basu S, Campbell H M, Dittel B N and Ray A 2010 Purification of specific cell population by fluorescence activated cell sorting (FACS) *J. Vis. Exp.* **41** e1546

[35] Albertson A J, Bohannon A S and Hablitz J J 2017 HCN channel modulation of synaptic integration in GABAergic interneurons in malformed rat neocortex *Front. Cell Neurosci.* **11** 109

[36] Ting J T, Lee B R, Chong P, Soler-Llavina G, Cobbs C, Koch C, Zeng H and Lein E 2018 Preparation of acute brain slices using an optimized N-methyl-D-glucamine protective recovery method *J. Vis. Exp.* **132** e53825

[37] Wu L G and Saggau P 1994 Presynaptic calcium is increased during normal synaptic transmission and paired-pulse facilitation, but not in long-term potentiation in area CA1 of hippocampus *J. Neurosci.* **14** 645–54

[38] Dobrunz L E and Stevens C F 1997 Heterogeneity of release probability, facilitation, and depletion at central synapses *Neuron* **18** 995–1008

[39] Lømo T 2003 The discovery of long-term potentiation *Phil. Trans. R. Soc.* A **358** 617–20

[40] Nicoll R A and Brief A 2017 History of long-term potentiation *Neuron* **93** 281–90

[41] Dawson W W and Wiederwohl H 1965 Functional alteration of visual receptor units and retinal pigments by x-irradiation *Radiat. Res.* **24** 292–304

[42] Pande K *et al* 2016 Femtosecond structural dynamics drives the trans/cis isomerization in photoactive yellow protein *Science* **352** 725–9

[43] Cannon K E *et al* 2019 LITE-1 mediates x-ray avoidance response in C. elegans *bioRxiv Preprint*

[44] Boyden E S, Zhang F, Bamberg E, Nagel G and Deisseroth K 2005 Millisecond-timescale, genetically targeted optical control of neural activity *Nat. Neurosci.* **8** 1263–8

[45] Lin J Y, Lin M Z, Steinbach P and Tsien R Y 2009 Characterization of engineered channel rhodopsin variants with improved properties and kinetics *Biophys. J.* **96** 1803–14

[46] Valais I, Michail C, David S, Nomicos C D, Panayiotakis G S and Kandarakis I 2008 A comparative study of the luminescence properties of LYSO:Ce, LSO:Ce, GSO:Ce and BGO single crystal scintillators for use in medical x-ray imaging *Phys. Med.* **24** 122–5

[47] Burdette M K *et al* 2019 Organic fluorophore coated polycrystalline ceramic LSO:Ce scintillators for x-ray bioimaging *Langmuir* **35** 171–82

[48] Spurrier M A, Melcher C L, Szupryczynski P, Yang K and Carey A A 2007 Effects of Ca2+ co-doping on the scintillation properties of LSO:Ce *Poster Presented At: IEEE Int. Conf. on Inorganic Scintillators and Their Applications*

[49] Wu Y, Koschan M, Foster C and Melcher C L 2019 Czochralski growth, optical, scintillation, and defect properties of cu^{2+} codoped $lu_2sio_5 : ce^{3+}$ single crystals *Cryst Growth Des.* **19** 4081–9

[50] Kushibiki T, Okawa S, Hirasawa T and Ishihara M 2014 Optogenetics: novel tools for controlling mammalian cell functions with light *Int. J. Photoenergy* **2014** 1–10

[51] Long M A and Fee M S 2008 Using temperature to analyse temporal dynamics in the songbird motor pathway *Nature* **456** 189–94
[52] Bushberg J T, Seibert J A, Leidholdt E M and Boone J M 2011 *The Essential Physics of Medical Imaging* 3rd edn (Philadelphia, PA: Lippincott Williams & Wilkins)
[53] Al-Juboori S I, Dondzillo A, Stubblefield E A, Felsen G, Lei T C and Klug A 2013 Light scattering properties vary across different regions of the adult mouse brain *PLoS One* **8** e67626
[54] Fischer M *et al* 2019 Biodistribution and inflammatory response of intracranial delivery of scintillating nanoparticles *bioRxiv Preprint*
[55] Gerstner H B, Orth J S and Richey E O 1955 Effect of high-intensity x-radiation on velocity of nerve conduction *Am. J. Physiol.* **180** 232–6
[56] Gerstner H B 1956 Effect of high-intensity x-radiation on the A group fibers of the frog's sciatic nerve *Am. J. Physiol.* **184** 333–7
[57] Lipetz L E 1955 The x-ray and radium phosphenes *Br. J. Ophthalmol.* **39** 577–98
[58] Fuglesang C, Narici L, Picozza P and Sannita W G 2006 Phosphenes in low earth orbit: survey responses from 59 astronauts *Aviat. Space Environ. Med.* **77** 449–52
[59] Sutton K A, Black P J, Mercer K R, Garman E F, Owen R L, Snell E H and Bernhard W A 2013 Insights into the mechanism of x-ray-induced disulfide-bond cleavage in lysozyme crystals based on EPR, optical absorption and x-ray diffraction studies *Acta Crystallogr.* D **69** 2381–94
[60] Groh V, Meyer J C, Panizzon R and Zortea-Caflisch C 1984 Soft X–irradiation influences the integrity of Langerhans cells. A histochemical and immunohistological study *Dermatologica* **168** 53–60
[61] Lacefield C O, Itskov V, Reardon T, Hen R and Gordon J A 2012 Effects of adult-generated granule cells on coordinated network activity in the dentate gyrus *Hippocampus* **22** 106–16
[62] Burghardt N S, Park E H, Hen R and Fenton A A 2012 Adult-born hippocampal neurons promote cognitive flexibility in mice *Hippocampus* **22** 1795–808
[63] Pazzaglia S, Briganti G, Mancuso M and Saran A 2020 Neurocognitive decline following radiotherapy: mechanisms and therapeutic implications *Cancers* **12** 146
[64] Casciati A *et al* 2016 Age-related effects of x-ray irradiation on mouse hippocampus *Oncotarget* **7** 28040–58
[65] Motomura K, Ogura M, Natsume A, Yokoyama H and Wakabayashi T 2010 A free-radical scavenger protects the neural progenitor cells in the dentate subgranular zone of the hippocampus from cell death after X-irradiation *Neurosci. Lett.* **485** 65–70
[66] Prager I, Patties I, Himmelbach K, Kendzia E, Merz F, Müller K, Kortmann R-D and Glasow A 2016 Dose-dependent short- and long-term effects of ionizing irradiation on neural stem cells in murine hippocampal tissue cultures: neuroprotective potential of resveratrol *Brain Behav.* **6** e00548
[67] George J, Giannoni L and Meng L J 2019 Energy-modulated x-ray fluorescence and luminescence emissions from therapeutic nanoparticles *Phys. Med. Biol.* **64** 035020
[68] Ronzitti E, Conti R, Zampini V, Tanese D, Foust A J, Klapoetke N, Boyden E S, Papagiakoumou E and Emiliani V 2017 Submillisecond optogenetic control of neuronal firing with two-photon holographic photoactivation of chronos *J. Neurosci.* **37** 10679–89
[69] Miyazaki T, Chowdhury S, Yamashita T, Matsubara T, Yawo H, Yuasa H and Yamanaka A 2019 Large timescale interrogation of neuronal function by fiberless optogenetics using lanthanide micro-particles *Cell Rep.* **26** 1033–1043.e5
[70] Lin X *et al* 2018 Core-shell-shell upconversion nanoparticles with enhanced emission for wireless optogenetic inhibition *Nano Lett.* **18** 948–56
[71] Berry R, Getzin M, Gjesteby L and Wang G 2015 X-optogenetics and U-optogenetics: feasibility and possibilities *Photonics* **2** 23–39
[72] Melcher C L and Schweitzer J S 1992 Cerium-doped lutetium oxyorthosilicate: a fast, efficient new scintillator *IEEE Trans. Nucl. Sci.* **39** 502–5
[73] Stratos D *et al* 2010 Evaluation of the co-doped LSO:Ce,Ca scintillator crystal in the x-ray energy range from 50 to 140 kVp for medical imaging applications *2010 IEEE Int. Conf. on Imaging Systems and Techniques* (IEEE) pp 253–5
[74] Berndt A, Schoenenberger P, Mattis J, Tye K M, Deisseroth K, Hegemann P and Oertner T G 2011 High-efficiency channel rhodopsins for fast neuronal stimulation at low light levels *Proc. Natl Acad. Sci. USA* **108** 7595–600
[75] Lin J Y 2011 A user's guide to channel rhodopsin variants: features, limitations and future developments *Exp. Physiol.* **96** 19–25
[76] Lempicki A and Glodo J 1998 Ce-doped scintillators: LSO and LuAP *Nucl. Instrum. Methods Phys. Res.* A **416** 333–44
[77] Fan L, Lin D, Zhang X, Shi Y, Zhang J, Xie J, Lei F and Zhang L 2016 Local structures of Lu atoms in a core shell approach for synthesis of Lu_2SiO_5 phase *Chem. Phys. Lett.* **644** 41–44
[78] Marshel J H *et al* 2019 Cortical layer-specific critical dynamics triggering perception *Science* **365** eaaw5202